An Improved and Fast MPPT Algorithm for PV Systems under Partially Shaded Conditions

Etezadinejad, Masoud ; Asaei, Behzad ; Farhangi, Shahrokh; Anvari-Moghaddam, Amjad

Published in:
I E E E Transactions on Sustainable Energy

DOI (link to publication from Publisher):
10.1109/TSTE.2021.3130827

Publication date:
2022

Document Version
Accepted author manuscript, peer reviewed version

An Improved and Fast MPPT Algorithm for PV Systems under Partially Shaded Conditions

Masoud Etezadinejad, Behzad Asaei, *Member, IEEE,* Shahrokh Farhangi, *Senior Member, IEEE,* and Amjad Anvari-Moghaddam, *Senior Member, IEEE*

***Abstract*—The use of solar power in some applications is challenging due to sudden changes in irradiance level and the fast occurrence of partial shading condition (PSC). For this reason, maximum power point tracking (MPPT) methods employed in photovoltaic (PV) applications allow for very fast detection and tracking of the maximum power point (MPP) during a partial shading condition. This fast reaction should minimize the power losses, have minimum steady-state oscillation and be accurate. In this paper, an analytical approach is proposed to track the real MPP in uniform irradiance condition (UIC) and PSC via the use of analytical formulas of the PV system behavior. The proposed method exhibits a rapid tracking speed, stable steady-state performance, and low sampling rate in all conditions. The characteristics and performance of the proposed algorithm under UIC and PSC are investigated and demonstrated through simulations and experimental tests.**

***Index Terms*—Fast MPPT, PV, Partial shading, Open circuit voltage (OCV), Analytical MPPT.**

I. Introduction

THE global approach towards reducing the consumption of fossil fuels is inciting industries to move towards green electrification [1]. Within converter design and manufacturing, the trend towards improving the tracking efficiency of the maximum power point tracking (MPPT) algorithms has resulted in numerous works on mitigating the risk of power losses due to partial shading conditions (PSC) and fast irradiance changes [2]-[4].

The majority of the PSC-compliant MPPT algorithms are based on the conventional MPPT algorithms like perturb and observe (P&O), incremental conductance (INC), direct MPPT algorithms, and soft computing-based algorithms, where some mechanisms added to the original algorithm to detect the occurrence of PSC and to track the global maximum power point (GMPP). Authors in [5] proposed a method to detect the PSC by monitoring the changes in the output power and while searching the whole array output in 0.8 fractions of module open-circuit voltage (OCV) to find the GMPP. In [6], an approach was utilized to substitute the original P&O reference voltage and check the local maximum power point (LMPP), which shows an acceptable performance under shading patterns. In [7] a method was introduced to estimate the position of the peaks to avoid time-consuming search for the local peaks using P&O method. In [8], soft computing methods have been combined with the traditional 0.8x OCV method to track the GMPP. One drawback is that the complexity of the introduced shading condition will become an issue for the implementation in large scale PV systems. In [9] 0.8xOCV method improved by restricting the search area and duty cycle sweep. Despite the effectiveness, the sweeping process may take time and lowers overall energy efficiency. One of the main critics of the OCV based methods is the fact that, despite the simplicity, the PV system's local peak power points during PSC does not always change in multiples of 0.8xOCV and there is a chance that a LMPP is ignored, especially in long PV arrays [8]. On the other hand, depending only on one variable such as OCV which is not constant in all working conditions might lead to the failure of the algorithm [10] and in fast climatic changes, the condition might be satisfied without the PSC [11].

Some efforts have been made to combine the conventional MPPT algorithms to benefit the advantages like simplicity and need for minimum hardware and mitigate the inherent problems of these algorithms, like the tradeoff between tracking speed and accuracy of the searched-based algorithms and the possibility of tracking failure in sharp irradiance changes [12] , [13]. In [14] a new algorithm using the Spline based-MPPT technique and P&O has been proposed, where it applies different duty cycles to the modules and samples the current and voltage. Despite the simplicity, the algorithm is not effective for fast-changing environments. In [15] a hybrid scheme has been introduced based on the particle swarm optimization (PSO) and P&O method to minimize the voltage search region. Apart from the semi-complex implementation of the algorithm, the algorithm shows large oscillation during the GMPP seeking procedure and a large part of the voltage region should be searched.

Many works have been dedicated to reduce the whole P-V search area and consequently, shorten the search time by establishing some rules to limit the search area. In [16], a maximum power trapezium area has been defined for the PV array to limit the search voltage area, which show fast and reliable performance. In [17], the authors tried to reduce the search range to minimize the computational burden. A triangular area has been defined using general statistical studies on the sample system. In [18], authors have also conducted a statistical study to determine the minimum and maximum voltage, and a further skipping procedure has been introduced.

M.Etezadinejad, B. Asaei, and S. Farhangi are with the School of Electrical and Computer Engineering, College of Engineering, University of Tehran, 14395/515, Tehran, Iran (m.etezadi@ut.ac.ir),

Amjad Anvari-Moghaddam is with the Department of Energy (AAU Energy), Aalborg University, 9220 Aalborg, Denmark (e-mail: aam@energy.aau.dk).

Two methods based on the INC method as GMPPT have been proposed in [19]. The first method is designed for small PV arrays, where the GMPP tacking process is excessively time-consuming, but results in high accuracy tracking. The second method designed specifically for long PV arrays, in which it compares the SC current of each PV module using the extra current sensor placed in the array where it purposed for the long PV arrays. The slow tracking speed and the extra current sensors make this method unattractive. Most of these algorithms still scan about 70% of the search voltage range of the whole P-V curve. Besides, the algorithm is relying on the outcome of a general statistical study on limited operating conditions of PV modules that might not cover all the possible scenarios, like considering the minimum irradiance of 100W/m^2 [4]. In addition, there should be extensive quantitative implementation to ensure that the assumed behavior is valid for all modules.

Model-based and direct algorithms are getting popular due to high accuracy and tracking speed and have been proposed in the literature. In [20], the authors proposed a new analytic GMPPT method where it tracks GMPPT using extensive mathematic formulations. After making an initial guess for the photon current, multiple equations should be solved for each string by iterative processes to track the GMPP. The big disadvantage of such a method is that there is no guarantee that all these equations will be converged to a correct answer. This will also become more complicated in an array with multiple PV strings, where the initial guess of all photon currents might affect the final answer and will put a lot of calculation load on the processor. The proposed algorithm in [21] has a simpler mathematical approach, but despite the effectiveness, the comparison of the final GMPP estimation shows a poor performance in terms of the tracking efficiency. The proposed algorithm in [22] does also suffers from low efficiency at some operation level, and the complexity makes it undesirable for fast-track applications. Authors in [23] used the dividing rectangles optimization algorithm to reach the GMPP, but it did not guarantee convergence to the GMPP and considerable energy losses are inevitable during the dividing procedure. The method in [24] uses the empirical expression of the voltage and current relation during PSC to estimate the location of the MPPs, but it fails to locate the GMPP with high efficiency in all conditions which makes it undesirable.

As briefly described in the review, many works dedicated to improve the tracking speed and efficiency of a GMPPT algorithms, but despite the progress made, most of the algorithms show drawbacks that make them undesirable for the PV application with fast irradiance changes (e.g., portable applications). The main drawback can be mentioned as slow tracking speed, power losses during search period and tracking failure. This paper proposed, designed, and implement a novel fast GMPPT algorithm by predominantly utilizing analytical MPPT and the mathematical effects of the PSC on the PV module and array behavior. The main focus is to be effective and efficient in the fast-changing environments. The shade detection method utilizes a two-step verification method to ensure the correct PSC detection and the operation voltage at each LMPP and for the GMPP are calculated using mathematical equations of the PV system. The proposed GMPPT algorithm is capable of locating all MPP fast and precise, with a very low steady-state oscillation. The rest of the paper is written as follows. In Section II, the PV model and the basic analytical formulas are presented and the effects of PSC on PV characteristics are investigated. Section III demonstrates the proposed algorithm principle and formulation. Section IV evaluates and demonstrates the performance of the proposed algorithm through simulations and experimental implementation and finally, Section V concludes the paper.

II. The PV Model and Basic Analytical Formulation

A. PV Module Model

One of the most known models for a solar cell is the single-diode model which is shown in Fig. 1. The relation between voltage and current of the cell can be extracted as follows:

$$I = I_{ph} - I_s\left(exp\left(\frac{V + R_s I}{aV_t}\right) - 1\right) - \frac{V + R_s I}{R_p} \quad (1)$$

where V and I represent cell's output voltage and current respectively, I_{ph} is the cell's generated current, R_s and R_p are cell's series and parallel parasitic resistances, respectively, V_t and a are the thermal voltage and the quality factor of diode p–n junction in the cell respectively, and I_s stands for cell's diode dark current.

B. MPPT Algorithm

The algorithm proposed in [25] has superior tracking characteristics like relative simplicity, high tracking efficiency, and fast racking during UIC. However, it is only effective for UIC and has to be modified to detect PSC and track the GMPP effectively. This section will provide the base MPPT algorithm according to [25].

By eliminating the effect of series and parallel resistors in (1), the V-I relation of an ideal PV cell can be written as:

$$I_i = I_{ph} - I_s\left(e^{\frac{V_i}{aV_t}}\right) + I_s \quad (2)$$

where I_i and V_i are ideal array voltage and current respectively. Neglecting the single I_s and multiplying (2) with V_i will yield the output power equation of an ideal solar cell.

$$P_i = V_i I_{ph} - V_i I_s\left(e^{\frac{V_i}{aV_t}}\right) \quad (3)$$

Knowing that the derivation of the power with respect to the voltage is zero at the MPP (e.g., LMPP in Fig. 2), yields:

$$\frac{dP}{dV_i} = I_{ph} - I_s e^{\frac{V_i}{aV_t}} - I_s\frac{V_i}{aV_t}e^{\frac{V_i}{aV_t}} = 0 \quad (4)$$

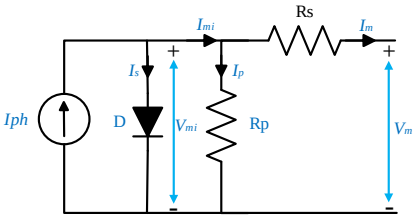

Fig. 1. Single diode equivalent circuit of a solar cell

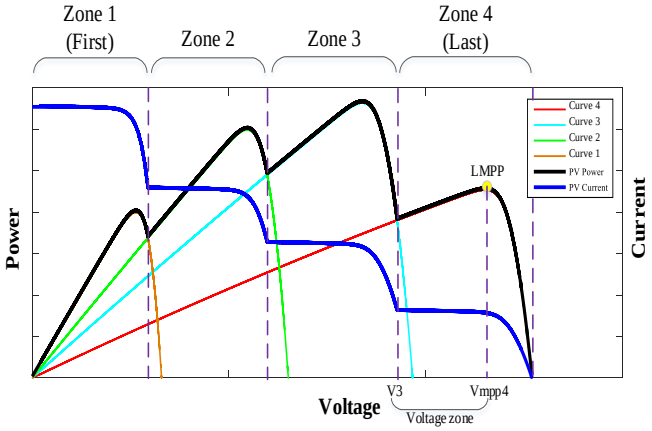

Fig. 2. Output characteristics and zone classification of four series connected modules receiving different irradiances.

(4) can be rewritten using some algebraic simplification as:

$$e^{\frac{V_{mi}}{aV_t}+1}\left(\frac{V_{mi}}{aV_t}+1\right)=\frac{I_{ph}}{I_s}e \tag{5}$$

Consequently, using LamberW function, the analytic equation for calculation of an ideal array voltage at MPP under a UIC is:

$$V_{mi}=aN_sV_t\left(W\left(\frac{I_{ph}}{I_s}e\right)+1\right) \tag{6}$$

where W is the LambertW function and N_s is the number of series-connected cells in an array [25]. The MPP voltage of an ideal solar array under UIC can be directly calculated using (6). By adding the effect of series and parallel resistances to (6) to have the MPP voltage of a solar cell using single diode model, the final equation for calculation of the MPP voltage of PV cell under UIC is written as (7).

$$V_m=V_{mi}-\left(I_{ph}-\frac{V_{mi}}{R_p}-I_s\left(e^{\frac{V_{mi}}{aV}}\right)\right)R_s \tag{7}$$

where V_m is the MPP voltage of a real PV cell. More details can be found in Appendix A.

I_s can be considered as a function of the cell temperature and can be calculated using module datasheet parameters [25] using (2):

$$I_s=\frac{I_{SCn}+k_i(T-T_c)}{exp\left(\frac{V_{OCn}+k_v(T-T_c)}{aV_t}\right)-1} \tag{8}$$

where I_{SCn} and V_{OCn} are the module's short circuit current and OCV at the standard test conditions (STC), k_v and k_i represent voltage and current temperature coefficients and T and T_c are working and STC temperatures of the module respectively. I_{ph} can be calculated directly from (1) by having a sample of V and I at any operation point [25]. Other parameters including V_t, a, I_s, R_s and R_p can be simply calculated using the available parameters estimation methods like [26] and the module's datasheet parameter. In regards to the sensitivity of the base algorithm, an analysis has been performed in [25].

The effect of temperature on (7) can be introduced in the MPPT through (8) using a temperature sensor. Due to the small size of the PV panels, it can be assumed that the temperature will not change as fast as the irradiance and a uniform temperature can be considered for the whole array and only one temperature sensor is utilized. Equation (7) can be re-written by considering the whole PV array, by introducing the number of series and parallel connected arrays as:

$$V_m=V_{mi}-\left(I_{ph}-\frac{V_{mi}}{\frac{N_i}{N_p}R_p}-I_s\left(e^{\frac{V_{mi}}{aN_iV}}\right)\right)\frac{N_i}{N_p}R_s \tag{9}$$

where V_m is the MPP voltage of a real PV array, N_i is the number of series connected modules in an array (or cells under each Bypass Diode (BD) in each module) and N_p is the number of parallel arrays. This should be noted the algorithm only needs to measure the voltage and current at the array level and will estimate the other parameters by changing the operating point voltage (OPV).

III. The Proposed MPPT Scheme

A. PSC and the Base Algorithm Behavior

When the base MPPT algorithm is exposed to a PSC, it always detects the LMPP of the last peak as the MPP. This is because all shaded and unshaded modules contribute in power supply in the last pea, where no BD is conducting in the last peak, and the N_i value in (9) does not change and indicates the full array. Assuming an array of 4 series connected modules, where each module is equipped with a single BD, and has N_t series connected cells. Each module receives different irradiances from G1 to G4 where G1 > G2 > G3 > G4. The output P-V curve of this condition will be similar to Fig. 2. The base algorithm will indicate a point in the voltage zone of Fig. 2 as the MPP since N_i in (9) is set to $4\times N_t$.

B. PSC Detection

Sharp irradiance changes will affect the array output current (and power). Monitoring the rate of change in array current and determining a threshold value is a simple and effective indicator to detect PSC. This condition is expressed as the following equation.

$$\varepsilon\le\left|\frac{I_{[N-1]}-I_{[N]}}{I_{[N]}}\right| \tag{10}$$

where ε is the threshold value, $I_{[N-1]}$ and $I_{[N]}$ are the measured array current at the [N-1]th and [N]th samples respectively. This should be noted that this is only the first step to realize a change in irradiance level, and the PSC will be confirmed using (11).

The value of ε should be chosen in such a way to cover all possible scenarios of irradiance change and meet the desired sensitivity. To the desirable value, A series of simulations have been performed on the test systems, with irradiances starting from 100W/m2 till 1200W/m2. Each irradiance has been applied to the panels of the test systems using the script, and the MPPs are tracked, and the change of the current is recorded.

TABLE I
RESULT OF NS VALUE CHANGE IN THREE DIFFERENT IRRADIANCE SCENARIOS USING KYOCERA KC200GT MODULE WITH ONE BD IN EACH MODULE

Irradiance Condition	Ns in (9)	Zone	Actual Power of LMPP	Before OCV update		After OCV update			
				Output by Using (9)	Tracking Efficiency	OCV Using (12)	OCV of Each Module	Output by Using (9)	Tracking Efficiency
Module A: 900W/m^2 Module B: 750W/m^2 Module C: 600W/m^2 Module D: 450W/m^2	54 54×2 54×3 54×4	1 2 3 4	179.7 W 314.4 W 391.7 W 402.9 W	179.7 W 312.2 W 368.9 W 377.3 W	100 % 99.3 % 97.1 % 95.6 %	32.71 64.92 96.28 126.36	32.71 32.21 31.36 30.08	179.7 W 314.2 W 391.4 W 402.8 W	100% 99.9% 99.9% 99.9%
Module A: 800W/m^2 Module B: 650W/m^2 Module C: 450W/m^2	54 54×2 54×3	1 2 3	159.2 W 272.4 W 296.2 W	159.2 W 268.1 W 282.4 W	100 % 98.4 % 96.3 %	32.49 64.41 94.75	32.49 31.92 30.34	159.2 W 272.2 W 296.2 W	100 % 99.9% 100 %
Module A: 900W/m^2 Module B: 650W/m^2	54 54×2	1 2	179.7 W 256.5 W	179.7 W 251.5 W	100 % 98.0 %	32.71 64.16	32.71 31.45	179.7 W 256.5 W	100 % 100 %

The results show that use of $\varepsilon = 0.05$ will be enough to cover the irradiances scenarios, as defined above. Regarding the first condition, it should also be noted that:

- The user does not need to calculate ε for each configuration and $\varepsilon = 0.05$ applies to all configurations,
- The desired sensitivity is in the way to avoid the normal current oscillation to satisfy first PSC detection condition,
- This condition will only realize that either sharp irradiance change or PSC has occurred, but to distinguish these conditions and avoiding unnecessary energy losses, a second condition has to be set.

When a PSC occurs, the base MPPT algorithm will always track a point where it falls in the voltage zone of Fig. 2. The voltage of the tracked point is always lower than the LMPP voltage of the last peak. This happens due to the fact that PSC will change the cells OCV. This is shown on Fig. 3. During an open circuit condition (OCC), the voltage across the diode is the same as OCV, and it can be calculated using (1).

$$V_D = aV_t \times ln\left(\frac{I_D + I_s}{I_s}\right) \quad (11)$$

where I_D is the current through the diode and V_D is the voltage across it. As all generated current, I_{ph}, will flow through the cell's diode in the OCC, any changes in the irradiance will change OCV. As shown in Fig. 3, the cell which is exposed to the higher irradiance will exhibit higher OCV. The OCV value in (9) is used with the assumption that all cells have uniform OCVs. However, as explained, the OCV value varies in the array under PSC. This difference causes a tracking error in the base algorithm. Fig. 4 depicts the P-V output of an array of four series connected modules is different UIC and PSC conditions, without bypass diodes. The results show that the OCV of the partially shaded array is different from the module under UIC. This will affect (2) and consequently, (9) calculates lower LMPP voltage than the actual LMPP voltage (voltage zone in Fig.2). Accordingly, the output power is less than the maximum available power of the last zone (LMPP point in Fig.2).

This behavior can be used as the second condition of the PSC detection procedure. After fulfilling (11), a voltage perturbation (ΔV) will be added to the OPV and if the output power increases, PSC occurrence can be confirmed. The value of the ΔV is considered as 1.5% of the whole array's OCV, following performing numerical studies on different PSC scenarios.

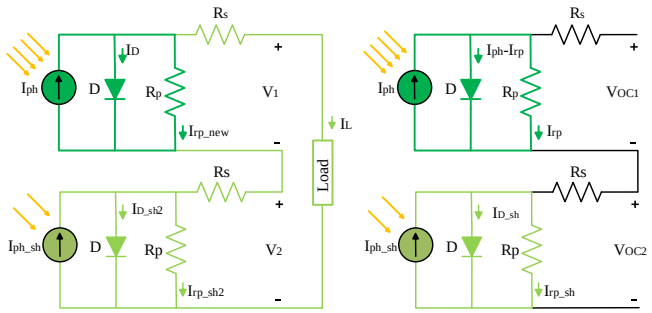

Fig. 3 Equivalent circuit of an array during PSC using a single-diode model. (a) Array connected to a load where both modules participate in load supply ($V_1 > V_2$). (b) Array in OCC ($V_{oc1} > V_{oc2}$).

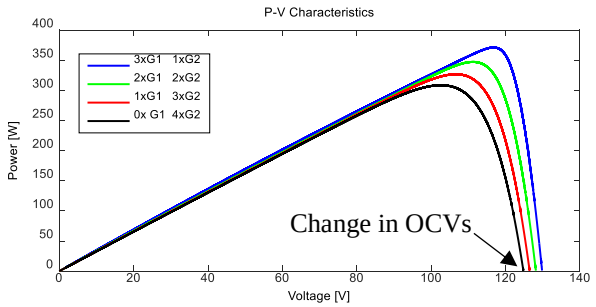

Fig. 4. Output characteristic of 4 series connected modules in UIC and different PSCs. Modules have no bypass diodes.

C. GMPPT Detection Procedure

The base MPPT algorithm can find the local MPPs by changing the respective number of series connected cells on each module in (9), N_i. In order to find the power of each LMPP, after PSC is confirmed by (11), the algorithm will change N_i value in (9) in multiples of the number of series connected modules, from the maximum value of series connected modules to 1.

Consequently, the OPV changes and the algorithm samples output power, voltage and current of each zone (LMPPs). Finally, by comparing the output power of each zone, the GMPP zone and corresponding N_i will be detected.

TABLE I shows the results of a numerical study on the efficiency of LMPP tracking, where an acceptable result is achieved. However, the accuracy of GMPPT is not good enough compared to the base MPPT algorithm since V_{OC} in (8) changes in the presence of PSC as explained. V_{OC} can be updated by measuring or calculating V_{OC} of each module. OCV measurement is not practical because it causes an interruption in system performance. Thus, a non-interrupting method should

be presented. Writing (1) in OCC yields

$$0 = I_{ph} - I_s\left(exp\left(\frac{V_{OC}}{N_i a V_t}\right) - 1\right) - \frac{V_{OC}}{R_p} \quad (12)$$

There are two ways to calculate V_{OC} ; the effect of the parallel resistance either can be neglected or LambertW function can be used for this purpose. For simplicity, the effects of parallel resistance and I_s are neglected and mathematical simplification will yield the analytical solution for calculation of OCV for each module by (13).

$$V_{OC} = aN_i V_t\, ln(\frac{I_{ph}}{I_s}) \quad (13)$$

Getting the right value in (13) needs no interruption or additional equipment while enabling us to estimate OCV in all operating conditions within acceptable accuracy. Therefore, when OPV is changing to find the GMPP, V_{OC} in each local peak can be calculated by (13) simultaneously. The OCV change in each zone is composed of two parts:

1. The result of a change in irradiance level.
2. The result of surplus current that flows through the internal diodes.

Assuming that there are *n* series connected modules forming an array. Each array is exposed to a different irradiance, and the i^{th} peak in the array's P-V curve is the GMPP. In order to calculate the OCV of the i^{th} module, (13) can be re-written as:

$$V_{OC_i} = aN_i V_t\, ln(\frac{I_{ph_{STC}}}{I_s} \times \frac{I_{ph_i}}{I_{ph_{STC}}}) = \underbrace{aN_i V_t\, ln(\frac{I_{ph_{STC}}}{I_s})}_{Voc_{STC}} + \underbrace{aN_i V_t\, ln(\frac{I_{ph_i}}{I_{ph_{STC}}})}_{\Delta V oc_i} \quad (14)$$

where V_{OC_STC} is the module OCV, I_{ph_STC} is the module's generated current at STC, V_{OC_i} and I_{ph_i} are the module OCV and generated current of the module in the i^{th} peak respectively, and ΔV_{OC_i} is the difference of OCV between the STC and the module in the i^{th} peak. Using (14), the ΔV_{OC_i} and consequently the V_{OC_i} at any irradiance condition can be calculated.

When the OPV is going to be at the i^{th} peak, surplus current effect in all (*i*-1) precedent modules should be taken into the account in V_{OC_i}. Thus, the surplus current effect in the i^{th} zone (ΔV_{Sur_i}) will be calculated by

$$\Delta V_{Sur_i} = \frac{\sum_{j=1}^{i} aN_i V_t\, ln(\frac{I_{ph_j}}{I_{ph_i}})}{i} \quad (15)$$

I_{ph} can be calculated at any point using (1). So, while the proposed algorithm is looking for the GMPP, it calculates and saves I_{ph} of all zones and all I_{ph_j} values are available. Finally, new OCV for calculating the GMPP of the i^{th} zone ($V_{OC\_new\_i}$) by considering the effect of irradiance change and surplus current can be calculated as follows:

$$V_{OC_{new_i}} = V_{OC_{STC}} + \Delta V_{OC_i} + \Delta V_{Sur_i} \quad (16)$$

The new calculated $V_{OC_{new_i}}$ will be used in (8) and consequently it will affect (9) for GMPP calculation. To further demonstrate the effectiveness of this procedure, the numerical simulations of TABLE I have been repeated, but this time OCV value of each zone is calculated and updated using (16). The result shows that, all LMPPs have been tracked in different conditions and the efficiency is well improved.

When the proposed algorithm works in GMPPT mode, PSC might be removed or changed to different structures. For the purpose of tracking the maximum available power, the PSC-detection conditions will be applied to the converter. The only difference is that the value of OCV has to be returned to the V_{OC_STC} after the satisfaction of the second PSC detection condition. The flowchart of the proposed algorithm is shown in Fig. 5.

IV. SIMULATIONS

In order to evaluate the performance of the proposed algorithm, two simulation studies in different working conditions are carried out on a PC with an Intel i5 - 2.5 GHz chip running Windows 7(64 bit) using MATLAB/Simulink.

The first simulation is performed in a simple PSC scenario exhibit the performance and the performance of the proposed method. The second simulation benchmark the performance of the proposed algorithm against some GMMPT algorithms proposed in [5], [7], [16] and the base MPPT algorithm in [25].

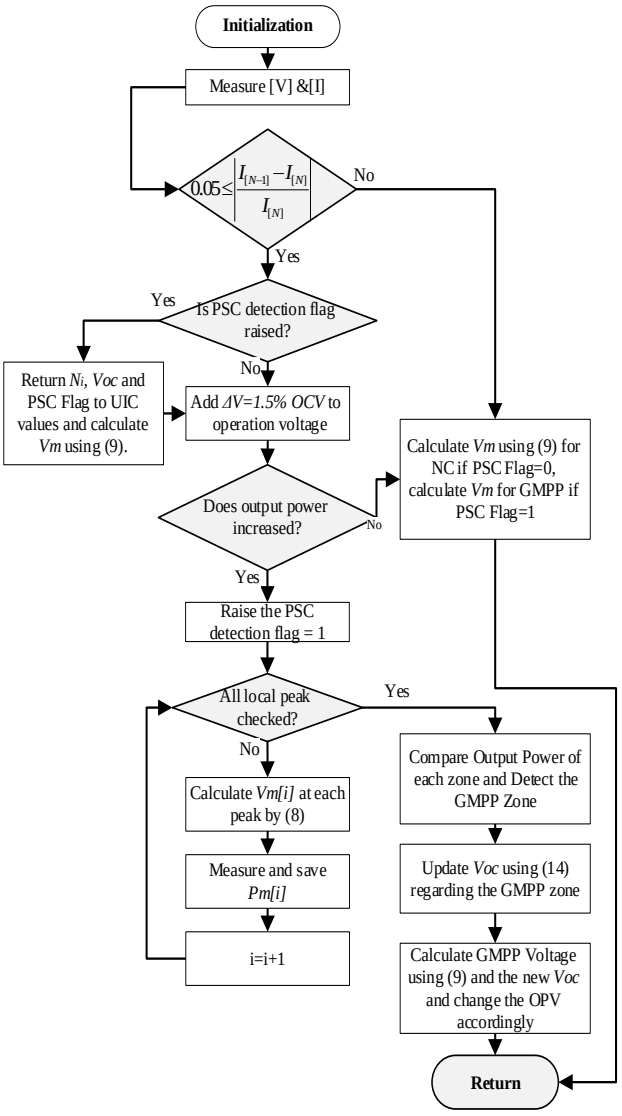

Fig. 5. Flowchart of the proposed GMPPT algorithm

For the purpose of the simulations, different irradiance conditions have been applied to the setup of 6 series connected HNM20P-12 Modules (each module has one BD), as depicted in Fig. 6. A boost converter is used to connect the array to the load and execute the algorithms, where the schematic configuration is shown on Fig. 6. The switching frequency is set to 33 kHz and the sampling frequency of the MPPT controller is 1 kHz for all simulation methods. The electrical parameters of HNM20P-12 module are extracted and shown on TABLE II.

A. *Simulation 1*

In this simulation case, at first, all arrays are under normal irradiance with an irradiance level of 1000 W/m2. Then at t=0.0495 s the irradiance condition changes to PSC according to Table III. Fig. 7. Provides the P-V curve of the first simulation with the steps taken to track the GMPP. Fig. 8 provides the trajectory of the array power, voltage and current through the simulation.

Cycle 1 (t=0.049s to 0.050s) The PSC takes place at t=0.0495s and the output power falls from P1 to P2. The algorithm gets the current sample at the end of S1 and the current shows 57% drop compared to previous sampling cycle (2.78A to 1.18 A), and the first PSC detection condition is satisfied. The algorithm initiates the second PSC confirmation condition by adding 1.5% of the OCV voltage (1.845V) to the previous OPV (95.62V), and the new OPV (97.465V) will be applied in the next cycle (S2).

Cycle 2 (t=0.050s to 0.051s): The output power increases from 112.5W to 114.5 W as result of adding 1.5% OCV to the OPV, and the second PSC condition is confirmed. Now the algorithm will initiate searching for the GMPP, and the OPV for the peak will be calculated using (9), and the calculated OPV will be applied in the next cycle (S3).

Cycle 3 to Cycle 6 (t=0.051s to 0.055s): The parameters corresponding to the 5th, 4th ,3rd and 2nd series-connected modules are stored in each cycle. The OPV is calculated using (9), and the calculated OPV will be applied in next cycle (S4).

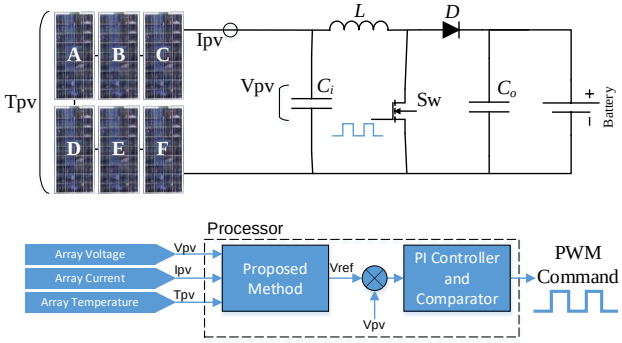

Fig. 6. Schematic of Boost DC/DC Converter structure and MPPT algorithm implementation in simulation environment. C_i=120 µF, C_o=480 µF, L=1300 µH

TABLE II:
SPECIFICATION OF HNM20P-12 MODULE

R_s	0.39 Ω	I_{mpp}	2.76 A	P_{mpp}	45 W
R_p	940 Ω	V_{mpp}	16.3 V	V_{OCn}	20.5 V
I_s	6.3E-8 A	N_s	36	I_{SCn}	2.98 A

TABLE III:
SIMULATION CONDITIONS

Simulation	Case	Time [s]	P_{GMPP} [W]	Irradiance condition	V_{GMPP} [V]	Module's irradiance [W/m^2]
1	1	Initial	270.3	UIC	97.3	A,B,C,D,E,F=1000
	2	t= 0.0495	144	PSC	68.1	A,B=1000, C,D=750, E,F=400
2	1	Initial	270.3	UIC	97.3	A,B,C,D,E,F=1000
	2	t_1=0.015	118.4	UIC	95.8	A,B,C,D,E,F=450
	3	t_2=0.025	112.2	PSC	66.0	A,B=700, C,D=600, E,F=300
	4	t_3=0.035	197.3	PSC	100.1	A,B,C,D=700, E,F=1000

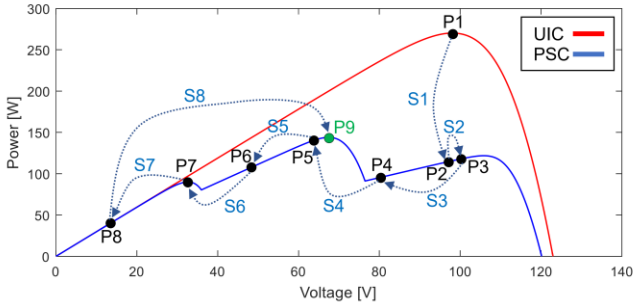

Fig. 7. P-V curve of each case in simulation 1, and the steps of GMPP tracking. Each P shows the operation point and each S represents 1 sampling cycle.

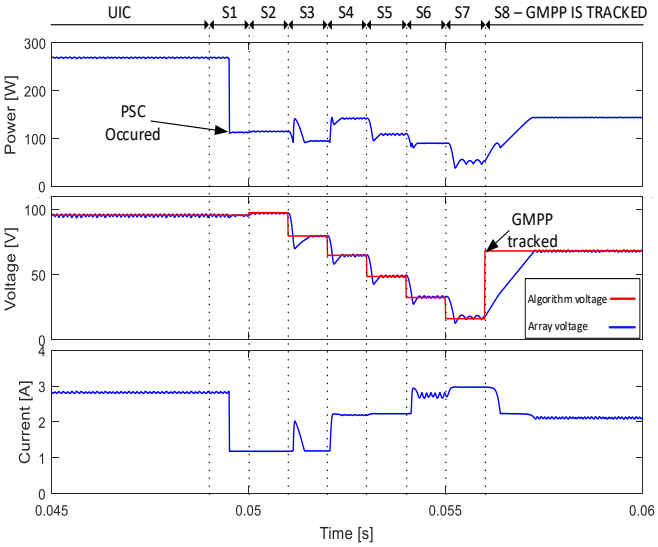

Fig. 8. Power, voltage and current results of Simulation 1

B. *Simulation 2*

The aim of this simulation is to assess the effectiveness of the proposed method compared to the existing methods (i.e., [5], [7], [16] and [25]) in terms of PSC detection, tracking accuracy and convergence speed under a PSC, and fast irradiance changes.

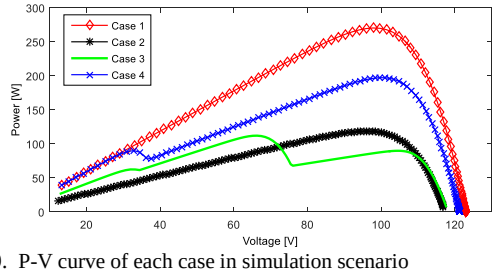

Fig. 9. P-V curve of each case in simulation scenario

The algorithm presented in [5] uses a 0.8 OVC method to search for the GMPP, and explores each single LMPP using INC method. As described in the literature review, [7] uses a current measurement approach to restrict the search area and increase the tracking speed while the approach outlined in [16] is based on a spline method which can track the GMPPT fast by limiting the search area. [25] is the base algorithm for the proposed method, and it is an analytical method only effective under UIC, as described in II-B. To do the comparative study, four different environmental conditions have been defined and the P-V curves of the simulated scenarios are shown in Fig. 9. The benchmarking results are also shown in Fig. 10.

Initially, all panels are exposed to UIC, and all methods are properly initiated to track the MPPT. The only difference between the tracking characteristics in this scenario is that the proposed algorithm in this work and the one in [25] exhibits very low steady state voltage oscillation, while those proposed in [5], [7] and [16] exhibit 3%, 5% and 2.2% steady-state oscillation, respectively.

The full simulation results can be found in TABLE IV. Below provides some highlights of the simulations:

- Irradiance change from case 1 to 2 satisfies the first PSC detection condition, but 1.5W output power reduction confirms that the array is under UIC.

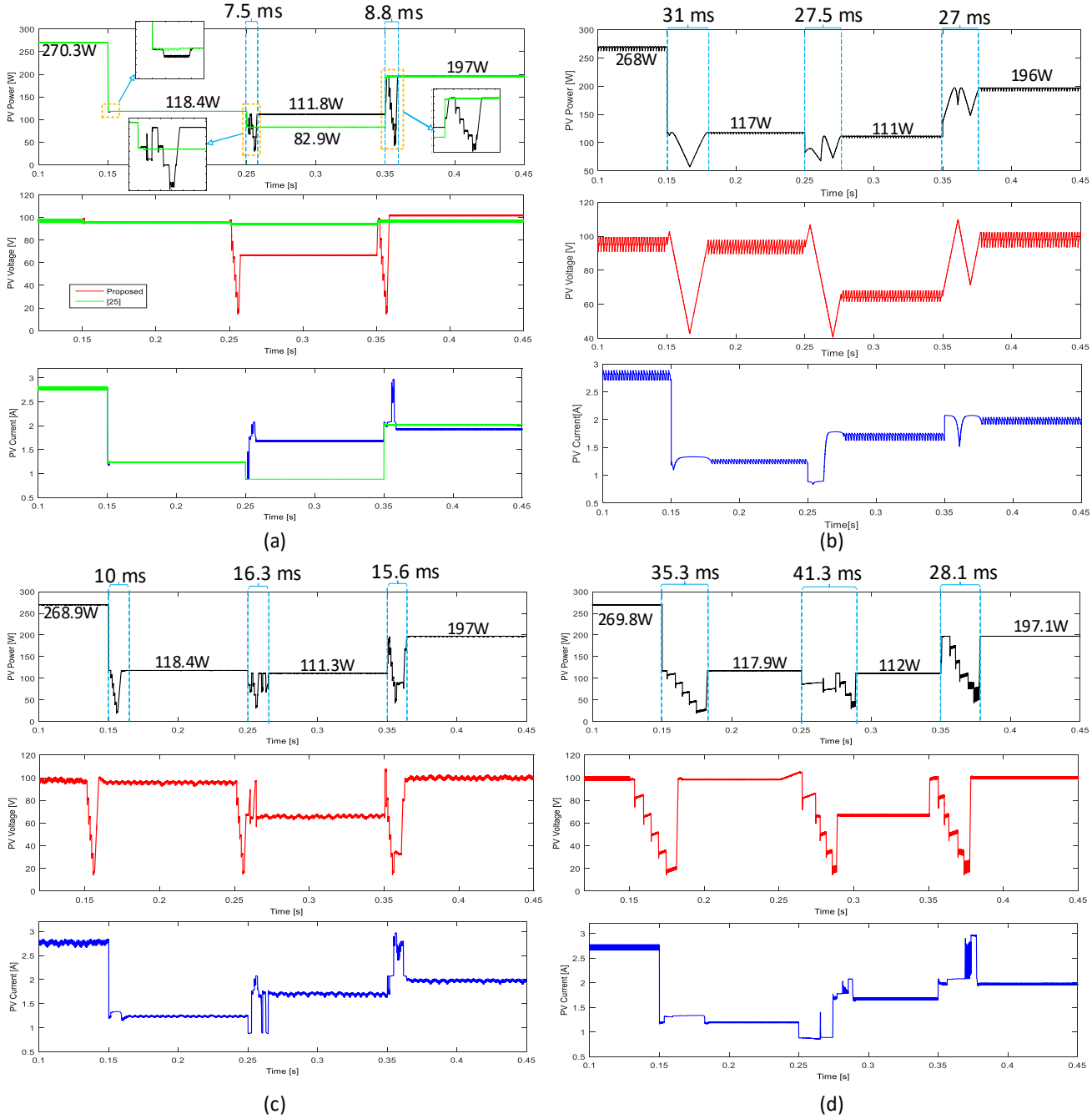

Fig. 10. Simulation results for power, voltage and current using different methods (a) the proposed method (black) and the basic method (green) as in [25] (b) method in [16] (c) method in [5], (d) method in [7]

- Algorithm [5] detects irradiance change (from Case 1 to 2) as PSC and initiates the search for the GMPP.
- During the irradiance changes from Case 2 to Case 3, the proposed algorithm measures 2W power increase following a check upon the second PSC test condition.
- During all simulations, [25] only indicates the last peak as the GMPP since it is only effective in UIC.
- [16] detects PSC correctly and limits the search area, but still, around 65% of the entire array is searched.
- [25] tracks the MPP for the normal condition with high accuracy, but it is an algorithm only for normal condition and cannot detect PSC. So, it fails to track the PSC in case 3. In case 4, since the algorithm always check the last peak and case 4 has the GMPP in the last peak, it detects the peak correctly, but since the OCV is not updated, the accuracy of the algorithm is much lower than the proposed method.
- The proposed algorithm only performs one measurement at each zone, while [5], [7] and [16] perform multiple measurements to provide input needed for the search-based methods.

TABLE IV
PERFORMANCE COMPARISON OF THE SIMULATED ALGORITHMS

Case	Algorithm	PGMPP [W]	Tracking time [ms]	Oscillating	Tracking efficiency	Correct PSC/UIC detection
1	Proposed	270.3	-	Low	100.00%	Y
	[5]	269.8	-	High	99.82%	Y
	[7]	268.9	-	High	99.48%	Y
	[16]	268.0	-	High	99.15%	Y
	[25]	270.3	-	Low	100.00%	Y
2	Proposed	118.4	1	Slight	99.96%	Y
	[5]	117.9	35.3	High	99.54%	N
	[7]	118.4	10	High	99.96%	N
	[16]	117.3	31	High	99.07%	Y
	[25]	118.4	1	Low	99.96%	Y
3	Proposed	111.8	7.5	Low	99.64%	Y
	[5]	112	41.3	High	99.82%	Y
	[7]	111.3	16.3	High	99.20%	Y
	[16]	111.5	27.5	High	99.38%	Y
	[25]	82.9	-	Low	73.80%	N
4	Proposed	197	8.8	Low	99.85%	Y
	[5]	197.1	28.1	High	99.90%	Y
	[7]	197.0	15.6	High	99.85%	Y
	[16]	196	27	High	99.34%	Y
	[25]	189	-	Low	95.70%	Y

These results prove the fast and accurate operation of the proposed algorithm in different PSC and UIC, but the other methods are considerably slower since they use search-based algorithm for the tracking. The biggest merit of the proposed algorithm is that it can track the MPP using the mathematical equations, which results in fast and accurate tracking.

V. EXPERIMENTAL RESULTS

The performance of the proposed algorithm is experimentally evaluated and benchmarked against the method of [16] using the set up shown in Fig. 11 under a rapid irradiance change. The setup includes a DC/DC boost converter equipped with the proposed algorithm, 4 x HNM20P-12 modules connected in series to form an array and a BD connected in parallel with each module. The converter is controlled using a PIC18F452 microcontroller that has a 10-bit ADC. The switching frequency of the converter is 32 kHz and sampling are done every 100 milliseconds for the proposed algorithm and every 5 milliseconds for [16]. The reason for the difference in the sampling is that [16] needs continuous change and the desirable performance couldn't be met with 1000ms sampling.

The temperature data is fed to the algorithm using LM335 temperature sensor. During the test, the arrays initially are under the UIC. Then, one of the arrays is shaded using a dark plastic film to create an I-V feature with two LMPPs, as shown in Fig. 11.(a). The P-V array specifications in UIC and PSC were extracted experimentally using manual point-to-point scanning and are shown in Fig. 12.

PSC occurrence causes 38% normalized current change and leads to second PSC detection test in the first sampling after PSC. It applies a perturbation step to the system OPV in the second sampling cycle which results in 6.1W output power increase. Note that the algorithm detects the PSC occurrence, scans and stores the LMPPs for the three operation points in the second, to fourth sampling cycles. The algorithm compares the saved values of power and carrying out the new OCV calculations. Power and voltage changes during the test are shown in Fig. 13, where it shows that the proposed algorithm tracks the PSC by only 4 samples of voltage and current after PSC occurrence, with a great steady state performance and efficiency, but [16] tracks the GMPP by 156 samples of voltage and current. The results are compared in TABLE V.

It is worthwhile to mention that the characteristics of the aged modules are not completely identical. Therefore, the characteristic is extracted from the datasheet parameters and this causes a slight estimation error.

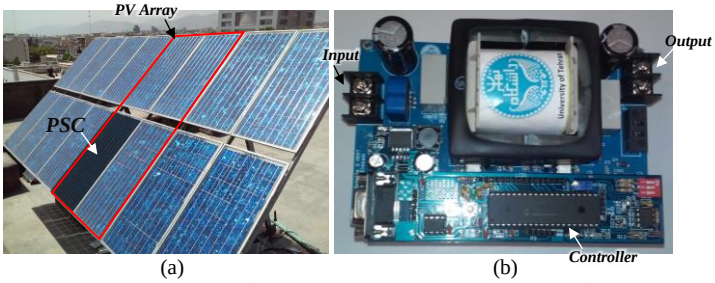

Fig. 11. Experimental setup for the proposed scheme. (a) Array configuration. (b) Solar MPPT.

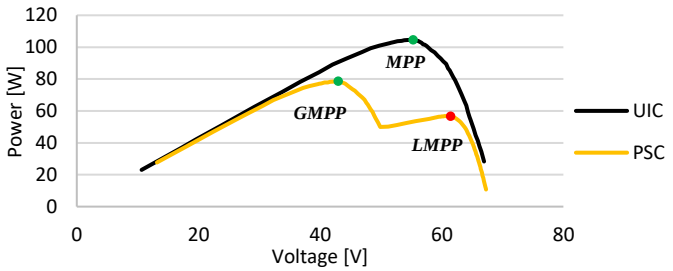

Fig. 12. Experimentally measured P–V characteristic of the PV array under UIC and PSC.

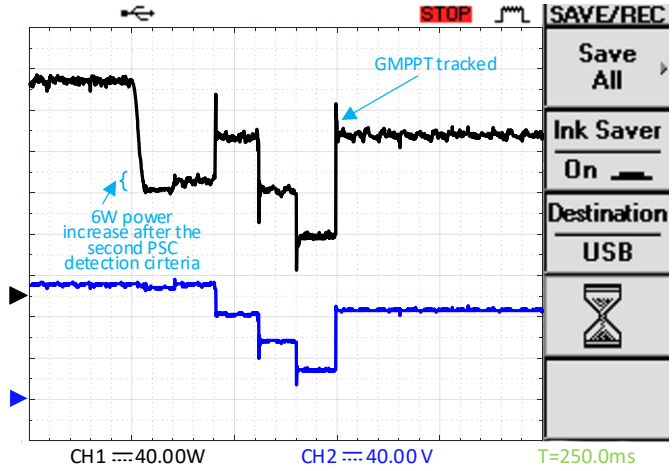

(a)

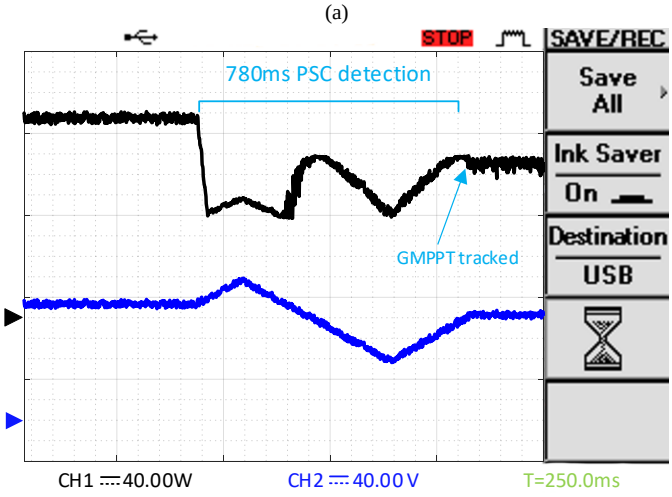

(b)

Fig. 13. Current and voltage profiles of the experimental results (a) the proposed algorithm (b) algorithm proposed in [16]

TABLE V
EXPERIMENTAL PERFORMANCES OF THE PROPOSED ALGORITHM AGAINST THE ONE PROPOSED IN [16]

Algorithm	Tracking efficiency at UIC	Tracking efficiency at PSC	Oscillating	Sampling rate	Number of V – I samples during PSC detection
Proposed	96%	97%	Slight	10 Hz	4
[16]	95%	96%	High	200 Hz	165

VI. CONCLUSION

This paper proposed an improved fast MPPT algorithm that is effective for both UIC and PSC, using the analytical expression of the PV cell algorithm and the effect of the PSC on the arrays output characteristics. The proposed method could scan the PV output using the analytical expression function, and find the GMPP. Moreover, the proposed method further improved the algorithm efficiency using an OCV update loop to compensate for the OCV mismatch between the shaded and unshaded arrays. The simulation results verified that the proposed method can reach the tracking efficiency of more than 99% on all simulation scenarios, and showed the best performance compared to other selected works. The simulation studies also substantiated the fast-tracking speed of the proposed algorithm where the search loss was reduced by more than 50% using a fast search method. Furthermore, the experimental implementation showed the simplicity of the algorithm and verified the algorithm performance.

Appendix A

The array voltage at MPP under a UIC is determined as follows:

$$V_{mi} = aN_sV_t\left(W\left(\frac{I_{ph}}{I_s}e\right)+1\right) \quad \text{(A-1)}$$

Fig. 1 shows V_{mi} and V_m. Kirchhoff's circuit law can be used to derive the equation for a solar cell using single diode model:

$$V_m = V_{mi} - R_sI_m \quad \text{(A-2)}$$

I_{mi} can be replaced using (2).

$$V_m = V_{mi} - R_s(I_{mi} - I_p) \quad \text{(A-3)}$$

$$V_m = V_{mi} - R_s\left(I_{mi} - \frac{V_{mi}}{R_p}\right) \quad \text{(A-4)}$$

$$V_m = V_{mi} - R_s\left(I_{ph} - I_s\left(e^{\frac{V_{mi}}{aV}}\right) + I_s - \frac{V_{mi}}{R_p}\right) \quad \text{(A-5)}$$

$$V_m = V_{mi} - R_s\left(I_{ph} - I_s\left(e^{\frac{V_{mi}}{aV}}\right) - \frac{V_{mi}}{R_p}\right) \quad \text{(A-6)}$$

REFERENCES

[1] REN21. 2020. Renewables 2020 Global Status Report (Paris: REN21 Secretariat).

[2] S. Silvestre, A. Boronat, A. Chouder, "Study of bypass diodes configuration on PV modules", Applied Energy, Volume 86, Issue 9, September 2009, Pages 1632-1640, ISSN 0306-2619.

[3] H. Patel and V. Agarwal, "MATLAB-Based Modeling to Study the Effects of Partial Shading on PV Array Characteristics," in IEEE Transactions on Energy Conversion, vol. 23, no. 1, pp. 302-310, March 2008.

[4] S. Hosseini, S. Taheri, M. Farzaneh and H. Taheri, "A High-Performance Shade-Tolerant MPPT Based on Current-Mode Control," in IEEE Transactions on Power Electronics, vol. 34, no. 10, pp. 10327-10340, Oct. 2019.

[5] H. Patel and V. Agarwal, "Maximum Power Point Tracking Scheme for PV Systems Operating Under Partially Shaded Conditions," in IEEE Transactions on Industrial Electronics, vol. 55, no. 4, pp. 1689-1698, April 2008.

[6] M. Aquib, S. Jain and V. Agarwal, "A Time-Based Global Maximum Power Point Tracking Technique for PV System," in IEEE Transactions on Power Electronics, vol. 35, no. 1, pp. 393-402, Jan. 2020.

[7] A. Ramyar, H. Iman-Eini and S. Farhangi, "Global Maximum Power Point Tracking Method for Photovoltaic Arrays Under Partial Shading Conditions," in IEEE Transactions on Industrial Electronics, vol. 64, no. 4, pp. 2855-2864, April 2017.

[8] Bi, J. Ma, K. L. Man, J. S. Smith, Y. Yue and H. Wen, "An Enhanced 0.8VOC-Model-Based Global Maximum Power Point Tracking Method for Photovoltaic Systems," in IEEE Transactions on Industry Applications, vol. 56, no. 6, pp. 6825-6834, Nov.-Dec. 2020.

[9] M. E. Başoğlu, "An Improved 0.8 VOC Model Based GMPPT Technique for Module Level Photovoltaic Power Optimizers," in IEEE Transactions on Industry Applications, vol. 55, no. 2, pp. 1913-1921, March-April 2019

[10] M. A. Ghasemi, H. M. Foroushani and M. Parniani, "Partial Shading Detection and Smooth Maximum Power Point Tracking of PV Arrays Under PSC," in IEEE Transactions on Power Electronics, vol. 31, no. 9, pp. 6281-6292, Sept. 2016.
[11] J. Ahmed and Z. Salam, "A Modified P&O Maximum Power Point Tracking Method With Reduced Steady-State Oscillation and Improved Tracking Efficiency," in IEEE Transactions on Sustainable Energy, vol. 7, no. 4, pp. 1506-1515, Oct. 2016.
[12] K. Hu, S. Cao, W. Li and F. Zhu, "An Improved Particle Swarm Optimization Algorithm Suitable for Photovoltaic Power Tracking Under Partial Shading Conditions," in IEEE Access, vol. 7, pp. 143217-143232, 2019.
[13] Zhang, D. Gamage, B. Wang and A. Ukil, "Hybrid Maximum Power Point Tracking Method Based on Iterative Learning Control and Perturb & Observe Method," in IEEE Transactions on Sustainable Energy, vol. 12, no. 1, pp. 659-670, Jan. 2021.
[14] A. Ostadrahimi and Y. Mahmoud, "Novel Spline-MPPT Technique for Photovoltaic Systems under Uniform Irradiance and Partial Shading Conditions," in IEEE Transactions on Sustainable Energy (Early acess), Ju;. 2020
[15] M. Kermadi, Z. Salam, J. Ahmed and E. M. Berkouk, "An Effective Hybrid Maximum Power Point Tracker of Photovoltaic Arrays for Complex Partial Shading Conditions," in IEEE Transactions on Industrial Electronics, vol. 66, no. 9, pp. 6990-7000, Sept. 2019.
[16] S. Xu, Y. Gao, G. Zhou and G. Mao, "A Global Maximum Power Point Tracking Algorithm for Photovoltaic Systems Under Partially Shaded Conditions Using Modified Maximum Power Trapezium Method," in IEEE Transactions on Industrial Electronics, vol. 68, no. 1, pp. 370-380, Jan. 2021.
[17] A. M. S. Furtado, F. Bradaschia, M. C. Cavalcanti and L. R. Limongi, "A Reduced Voltage Range Global Maximum Power Point Tracking Algorithm for Photovoltaic Systems Under Partial Shading Conditions," in IEEE Transactions on Industrial Electronics, vol. 65, no. 4, pp. 3252-3262, April 2018.
[18] M. Kermadi, Z. Salam, J. Ahmed and E. M. Berkouk, "A High-Performance Global Maximum Power Point Tracker of PV System for Rapidly Changing Partial Shading Conditions," in IEEE Transactions on Industrial Electronics, vol. 68, no. 3, pp. 2236-2245, March 2021.
[19] Wang, Y. Li and X. Ruan, "High-Accuracy and Fast-Speed MPPT Methods for PV String Under Partially Shaded Conditions," in IEEE Transactions on Industrial Electronics, vol. 63, no. 1, pp. 235-245, Jan. 2016.
[20] Y. Mahmoud and E. F. El-Saadany, "Fast Power-Peaks Estimator for Partially Shaded PV Systems," in IEEE Transactions on Energy Conversion, vol. 31, no. 1, pp. 206-217, March 2016.
[21] A. Xenophontos and A. M. Bazzi, "Model-Based Maximum Power Curves of Solar Photovoltaic Panels Under Partial Shading Conditions," in IEEE Journal of Photovoltaics, vol. 8, no. 1, pp. 233-238, Jan. 2018.
[22] M. Arjun, V. V. Ramana, R. Viswadev and B. Venkatesaperumal, "An Iterative Analytical Solution for Calculating Maximum Power Point in Photovoltaic Systems Under Partial Shading Conditions," in IEEE Transactions on Circuits and Systems II: Express Briefs, vol. 66, no. 6, pp. 973-977, June 2019.
[23] T. L. Nguyen and K. Low, "A Global Maximum Power Point Tracking Scheme Employing DIRECT Search Algorithm for Photovoltaic Systems," in IEEE Transactions on Industrial Electronics, vol. 57, no. 10, pp. 3456-3467, Oct. 2010.
[24] S. Moballegh and J. Jiang, "Modeling, Prediction, and Experimental Validations of Power Peaks of PV Arrays Under Partial Shading Conditions," in IEEE Transactions on Sustainable Energy, vol. 5, no. 1, pp. 293-300, Jan. 2014.
[25] G. Farivar, B. Asaei and S. Mehrnami, "An Analytical Solution for Tracking Photovoltaic Module MPP," in IEEE Journal of Photovoltaics, vol. 3, no. 3, pp. 1053-1061, July 2013.
[26] G. Farivar and B. Asaei, "A New Approach for Solar Module Temperature Estimation Using the Simple Diode Model," in IEEE Transactions on Energy Conversion, vol. 26, no. 4, pp. 1118-1126, Dec. 2011.

Masoud Etezadinejad received the B.Sc. degree in electrical engineering from the Iran University of Science and Technology in 2011 and the M.Sc. degree in electrical engineering from the University of Tehran in 2014. He is currently with Ørsted Wind Power, Fredericia, as senior power system engineer. His main research interests include offshore wind transmission systems design and control, techno-economical system optimization, data-driven approach for power system control and stability and energy management systems.

Behzad Asaei received his B.Sc. and M.Sc. degrees from the University of Tehran in 1988 and 1990, respectively, and his Ph.D. degree from Sydney University in 1995, all in electrical engineering. Since 2006, he has been at the University of Tehran, School of Electrical and Computer Engineering, where he is an Associate Professor and director of the Energy and Automotive Technology Lab. He has been managing several companies in the field of Automotive and Energy through his career. His research is focused on the field of automotive electronics, renewable energy project development, electric and hybrid electric vehicles, power electronics, motor drives, and power generation in which several projects have been completed.

Shahrokh Farhangi received the B.Sc., M.Sc., and Ph.D. degrees in electrical engineering from the University of Tehran, Iran, with (Hons.). He is currently a Professor at the School of Electrical and Computer Engineering, University of Tehran. His research interests include the design and modeling of power electronic converters, drives, photovoltaics, and renewable energy systems. He has managed many research and industrial projects, which some of which have won national and international awards. He has been selected as the Distinguished Engineer in Electrical Engineering by the Iran Academy of Sciences, in 2008.

Amjad Anvari-Moghaddam (S'10–M'14–SM'17) received the Ph.D. degree (Hons.) from University of Tehran in 2015 in Power Systems Engineering. From 2015 until 2019 he was a Postdoctoral Research Fellow at Aalborg University. Currently, he is an Associate Professor and Leader of Intelligent Energy Systems and Flexible Markets (iGRIDS) Research Group at the Department of Energy (AAU Energy), Aalborg University where he is also acting as the Vice-Leader of Power Electronic Control, Reliability and System Optimization (PESYS) and the coordinator of Integrated Energy Systems Laboratory (IES-Lab). His research interests include planning, control and operation management of microgrids, renewable/hybrid power systems and integrated energy systems with appropriate market mechanisms. He has (co)authored more than 260 technical articles, five books and nine book chapters in the field. Dr. Anvari-Moghaddam serves as the Associate Editor of the IEEE TRANSACTIONS ON POWER SYSTEMS, IEEE ACCESS, IEEE SYSTEMS JOURNAL, IEEE OPEN ACCESS JOURNAL OF POWER AND ENERGY, and IEEE POWER ENGINEERING LETTERS. He is the Vice-Chair of IEEE-PES Danish Chapter and serves as a Technical Committee Member of several IEEE PES/IES/PELS and CIGRE working groups. He was the recipient of 2020 DUO – India Fellowship Award, DANIDA Research Fellowship grant from the Ministry of Foreign Affairs of Denmark in 2018, IEEE-CS Outstanding Leadership Award 2018 (Halifax, Nova Scotia, Canada), and the 2017 IEEE-CS Outstanding Service Award (Exeter-UK).